

ADAPTIVE ANTENNA ARRAYS FOR CELLULAR CDMA COMMUNICATION SYSTEMS

Yiping Wang and J. R. Cruz

CSPLab, School of Electrical Engineering, The University of Oklahoma
Norman, OK 73019, USA

ABSTRACT

The use of an adaptive antenna array at the base station in the reverse link of cellular communication systems is proposed. Two kinds of adaptive methods are considered. First, the recursive least squares (RLS) algorithm, which is a reference signal based method, is used to adjust the weight coefficients of the array. For eigenstructure based methods, the ESPRIT algorithm is used for angle of arrival (AOA) estimation and the linear least squares estimate (LLSE) is used to determine the adaptive array weights. The improvement in performance is quantified by comparison with the omnidirectional antenna system using realistic simulations. The comparisons of different adaptive arrays are discussed and analyzed.

1. INTRODUCTION

Adaptive antenna arrays have been proposed as a technique to suppress interference and increase system capacity [1], [2]. The least-mean-square (LMS) adaptive algorithm has been commonly used to update the combining weights of adaptive antenna arrays [3], [4]. However, its slow convergence presents an acquisition and tracking problem for cellular systems. The direct matrix inversion (DMI) algorithm [5] has been proposed because of its fast convergence, however it is too computationally complex. Ohgane [6] considered the constant modulus adaptive algorithm (CMA) in time division multiple access (TDMA) mobile radio systems. This algorithm, however, is not well suited for code division multiple access (CDMA) systems because of power control. We propose the use of RLS [7] and ESPRIT based adaptive arrays to increase the user capacity of a CDMA cellular system. Our work differs from Liberti and Rappaport [1] in that we include the adaptive algorithm and consider the effect of all users in the central cell and all adjacent cells in the adaptation process. In [1], the results were obtained for an ideal given array pattern, whereas our results are more realistic and therefore more useful in predicting actual system performance.

2. BACKGROUND

We consider a four-element array at the base station where the sampled data \mathbf{x} is given by

$$\mathbf{x} = \mathbf{s} + \mathbf{i} + \mathbf{n} \quad (1)$$

where \mathbf{s} , \mathbf{i} and \mathbf{n} are the array sampled data column vectors of the desired signal, other users' interference signals and white noise. The white noise term is negligible if the number of users is large.

2.1. RLS Adaptive Arrays

The RLS adaptive algorithm is used to find a weight vector $\mathbf{w} = (w_1, w_2, w_3, w_4)$ such that the array can steer a beam in a desired direction. The iterative relations [8] are

$$\mathbf{P}(k+1) = \frac{1}{\alpha} \left\{ \mathbf{P}(k) - \frac{\mathbf{P}(k)\mathbf{x}^*(k+1)\mathbf{x}^T(k+1)\mathbf{P}(k)}{\alpha + \mathbf{x}^T(k+1)\mathbf{P}(k)\mathbf{x}^*(k+1)} \right\} \quad (2)$$

$$e(k+1) = r(k+1) - \mathbf{w}^T(k)\mathbf{x}(k+1) \quad (3)$$

$$\mathbf{w}(k+1) = \mathbf{w}(k) + \frac{\mathbf{P}(k)\mathbf{x}^*(k+1)}{\alpha + \mathbf{x}^T(k+1)\mathbf{P}(k)\mathbf{x}^*(k+1)} e(k+1) \quad (4)$$

where α is the forgetting factor and $r(k)$ is a desired reference signal. Equations (2)-(4) are started by adopting an initial guess for the weight vector $\mathbf{w}(0)$ and the initial Hermitian matrix $\mathbf{P}(0)$. It is common practice to select as an initial weight vector $\mathbf{w}(0) = [1, 0, 0, 0]$, thereby obtaining an omnidirectional array pattern (the antenna elements each have omnidirectional patterns) and to select $\mathbf{P}(0)$ as the identity matrix.

The adaptive array output signal $y(k)$ can be written as

$$y(k) = \mathbf{w}^T(k)\mathbf{x}(k). \quad (5)$$

Assume that the array elements are arranged in the xy -plane. Each of the four elements is located at the position $\mathbf{p}_i (i=1, 2, 3, 4)$. The angle is the plane wave normal projection angle. The unit vector in the positive y -axis direction has $\theta=0$. We define the slowness vector as

$$\alpha_0 = \frac{2\pi}{\lambda} \begin{bmatrix} \sin \theta \\ \cos \theta \end{bmatrix}$$

where λ is the wavelength of the propagation wave. The array pattern is given by [8]

$$G(\theta) = \frac{1}{4} \sum_{i=1}^4 w_i^* e^{-j\alpha_0^T \mathbf{p}_i}$$

2.2. ESPRIT Adaptive Arrays

In ESPRIT adaptive arrays, the ESPRIT algorithm is used for angle of arrival (AOA) estimation and the linear least squares estimate (LLSE) is used to determine the adaptive array weights [9].

ESPRIT is known to be one of the best high resolution methods for the estimation of angles of arrival. Unfortunately, the algorithm works only if the number of array elements is greater than the number of signals. In mobile communication systems, the number of user signals will far exceed the number of array elements. In order to use ESPRIT in conjunction with CDMA systems, we correlate the array outputs with the PN code of the desired user to despread the desired signal. We generate a signal at the PN code rate by holding the despread sample value for the chip length. Because of the excellent characteristics of the PN code, the data can be considered as consisting of only one signal and noise after despreading. This allows us to use ESPRIT.

A uniform linear array (ULA) of identical elements is considered with ESPRIT. The total least-squares ESPRIT algorithm [9] for AOA estimation is as follows:

(i) Obtain a covariance estimate $\tilde{\mathbf{R}}_{zz}$, from the despread data.

(ii) Compute the eigendecomposition of $\tilde{\mathbf{R}}_{zz}$

$$\tilde{\mathbf{R}}_{zz} \tilde{\mathbf{E}} = \tilde{\mathbf{E}} \mathbf{\Lambda}$$

where $\mathbf{\Lambda} = \text{diag}\{\lambda_1, \dots, \lambda_M\}$, $\lambda_1 \geq \dots \geq \lambda_M$, and $\tilde{\mathbf{E}} = [\mathbf{e}_1 | \dots | \mathbf{e}_M]$, M is the total number of sensors.

(iii) Obtain the signal subspace estimate

$$\mathbf{E}_z \stackrel{\text{def}}{=} \mathbf{e}_1 = \begin{bmatrix} \mathbf{E}_0 \\ \mathbf{E}_1 \end{bmatrix}.$$

(iv) Compute the eigendecomposition ($\lambda_1 > \lambda_2$),

$$\mathbf{E}_{01}^H \mathbf{E}_{01} \stackrel{\text{def}}{=} \begin{bmatrix} \mathbf{E}_0^H \\ \mathbf{E}_1^H \end{bmatrix} [\mathbf{E}_0; \mathbf{E}_1] = \mathbf{V} \mathbf{\Lambda} \mathbf{V}^H,$$

and partition \mathbf{V} into 1×1 submatrices,

$$\mathbf{V} \stackrel{\text{def}}{=} \begin{bmatrix} V_{11} & V_{12} \\ V_{21} & V_{22} \end{bmatrix}.$$

(v) Calculate the eigenvalue and eigenvector of $\Psi = -V_{12} V_{22}^{-1}$, denoted $\hat{\phi}$, and e_ϕ .

(vi) Estimate the AOA, $\hat{\theta} = \arcsin \left\{ c \arg \left(\hat{\phi} \right) / \omega_0 d \right\}$, where d is the distance between contiguous elements, ω_0 is the carrier frequency, c is the speed of propagation.

The array weight vector, which can be estimated by LLSE, is written as [9]

$$\mathbf{w} = \mathbf{E}_z [\mathbf{E}_z^H \mathbf{E}_z]^{-1} e_\phi. \quad (6)$$

2.3. BER Performance

In cellular mobile communication systems, the interference comes not only from co-users in the same cell but also from users in adjacent cells. To consider the effect of adaptive antenna arrays when CDMA users are simultaneously active in the central cell and all adjacent cells, we use the bit error rate (BER) expressions in [1]. For an omnidirectional antenna system,

$$P_b = Q \left(\sqrt{\frac{3N}{K(1+8\beta)-1}} \right), \quad (7)$$

and for an adaptive array system,

$$P_b = Q \left(\sqrt{\frac{3ND}{K(1+8\beta)-1}} \right) \quad (8)$$

where $Q(Y)$ is the standard Q-function, the probability that $y > Y$ when y is a zero-mean, unit variance, Gaussian distributed random variable; N is the processing gain, K is the number of users in one cell, $\beta = 0.05513$, and D is the directivity of the beam with pattern $G(\theta)$

$$D = \frac{2\pi}{\int_{-\pi}^{\pi} |G(\theta)|^2 d\theta}.$$

3. SIMULATION RESULTS

To demonstrate the performance of the RLS and ESPRIT adaptive arrays in a CDMA cellular system, computer simulations were performed. The data transmission rate for each user was 9600 b/s and the transmission bandwidth was $W = 1.25$ MHz. Each user was assigned a unique spreading sequence from a set of 129 Gold sequences of length 127, so the processing gain $N = 127$. We set all received signal powers equal, i.e., assume perfect power control.

3.1. RLS Results

The RLS adaptive antenna array was simulated for both uniform linear and circular arrays. The positions of the four array elements are, (a) uniform linear array: $\mathbf{p}_1 = (0, 0)^T$, $\mathbf{p}_2 = (-\frac{\lambda}{2}, 0)^T$, $\mathbf{p}_3 = (-\lambda, 0)^T$, $\mathbf{p}_4 = (-\frac{3\lambda}{2}, 0)^T$, and (b) uniform linear array: $\mathbf{p}_1 = (-\frac{\lambda}{2\sqrt{2}}, 0)^T$, $\mathbf{p}_2 = (0, -\frac{\lambda}{2\sqrt{2}})^T$, $\mathbf{p}_3 = (-\frac{\lambda}{2\sqrt{2}}, 0)^T$, $\mathbf{p}_4 = (0, \frac{\lambda}{2\sqrt{2}})^T$. The forgetting factor in the RLS algorithm was set to one.

An example of the array patterns obtained with six simultaneous users was simulated. The desired signal was

Table 1. Users' parameters for simulation

	User #1	User #2	User #3	User #4	User #5	User #6
Phase Shift (rad)	0	1.0472	1.5708	3.1416	0.5236	0.7854
Path Delay (μ s)	0	1.6280	0.8140	1.6280	2.4420	3.2560
Arrival Angle (rad)	0	0.7854	1.5708	0.5236	1.0472	-0.7854

user #1. All other simulation parameters are given in Table 1.

Using the RLS algorithm to adapt the array weights the algorithm converged to a steady-state solution after approximately 10 chips (10/127 data bits) for the linear array (Fig.1 (a)), and after approximately 20 chips (20/127 data bits) for the circular array (Fig.1 (b)). The array patterns after convergence are shown in Fig. 2. Notice that the adaptive arrays have steered the beam in the desired direction and placed nulls in the directions of the interference arrivals. The interference suppression varies between 11 dB and 19 dB for the linear array, and between 8 dB and 20 dB for the circular array. From Fig. 2, we can see that the linear array has a narrower beamwidth than the circular array. However, the uniform linear array exhibits a pattern which is symmetric about its axis.

Equation (7) was used to calculate the BER of the omnidirectional antenna system. For the adaptive array system, we first used the RLS algorithm to adapt the array with all the users' signals in the central cell and eight adjacent cells, for instance, if there were 100 users in the central cell and 800 users in all adjacent cells, then the adaptation was executed with one desired user and 899 interfering users. After that, (8) was used to get the BER. This simulation was carried out for every user in the central cell and the resulting bit error rates were averaged. Fig. 4 shows the results for the omnidirectional antenna system, uniform linear and circular array systems. At $P_e=10^{-2}$, the capacity improvement for the linear and circular array systems is more than 32% and 60%, respectively. Furthermore, increasing the array size leads to larger capacity improvements.

3.2. ESPRIT Results

The ESPRIT adaptive antenna array was simulated for the uniform linear array. The location of the four elements is the same as in the RLS array. Subarray 1 consists of elements #1, #2, and #3, and subarray 2 consists of elements #2, #3, and #4. Therefore, the total number of sensors is six.

An example of the array patterns is given in Fig. 3. This was obtained with the same simulation parameters as the RLS array. Notice that the performance improves as the data block size increases. Compared with the RLS array, the ESPRIT array has a narrower beamwidth, leading to better BER performance. The results of BER simulation

with two bit blocks of data have confirmed the improvement (Fig.4). At $P_e=10^{-2}$, the capacity improvement for the ESPRIT array system is more than 100% over the omnidirectional antenna system. However, this improvement comes at a price in computational requirements.

4. CONCLUSIONS

It can be concluded that the use of adaptive antenna arrays at the base station can significantly increase the capacity of CDMA cellular communication systems. In this paper, our simulation did not include the effects of multipath. But the approach can be used to include a multipath model. In our system, we did not consider antenna sectorization or voice activity detection. Inclusion of these techniques would further increase the system capacity.

REFERENCES

- [1] J. C. Liberti, Jr. and T. S. Rappaport, "Analytical results for reverse channel performance improvements in CDMA cellular communication systems employing adaptive antennas," *IEEE Trans. Veh. Technol.*, vol. 43, no. 3, pp. 680-690, Aug. 1994.
- [2] A. F. Naguib, A. Paulraj, and T. Kailath, "Capacity improvement with base-station antenna arrays in cellular CDMA," *IEEE Trans. Veh. Technol.*, vol. 43, no. 3, pp. 691-698, Aug. 1994.
- [3] B. Widrow, P. E. Mantey, L. J. Griffiths, and B. B. Goode, "Adaptive antenna systems," *Proc. IEEE*, vol. 55, pp. 2143-2159, Dec. 1967.
- [4] R. T. Compton Jr., "An adaptive array in a spread-spectrum communication system," *Proc. IEEE*, vol. 66, pp. 289-298, March 1978.
- [5] J. H. Winters, "Signal acquisition and tracking with adaptive arrays in wireless systems," in *Proc. IEEE 43rd Vehicular Technology Conf*, pp. 85-88, 1993.
- [6] T. Ohgane, "Characteristics of CMA adaptive array for selective fading compensation in digital land mobile radio communications," *Electron. and Commun. in Japan*, vol. 74, Part 1, pp. 43-53, 1991.
- [7] Y. Wang, and J. R. Cruz, "Adaptive antenna arrays for the reverse link of CDMA cellular communication systems," *Electron. Letters*, vol. 30, no. 13, pp. 1017-1018, June 1994.
- [8] D. E. Dudgeon, and R. M. Mersereau, *Multidimensional digital signal processing*, Englewood Cliffs, NJ: Prentice-Hall, 1984.
- [9] R. Roy, and T. Kailath, "ESPRIT-estimation of signal parameters via rotational invariance techniques," *IEEE Trans.*

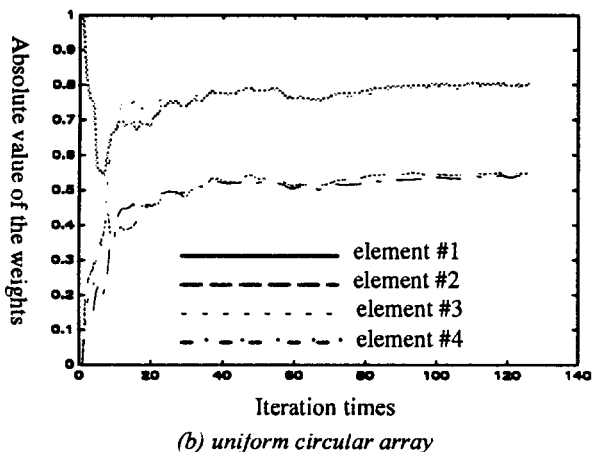
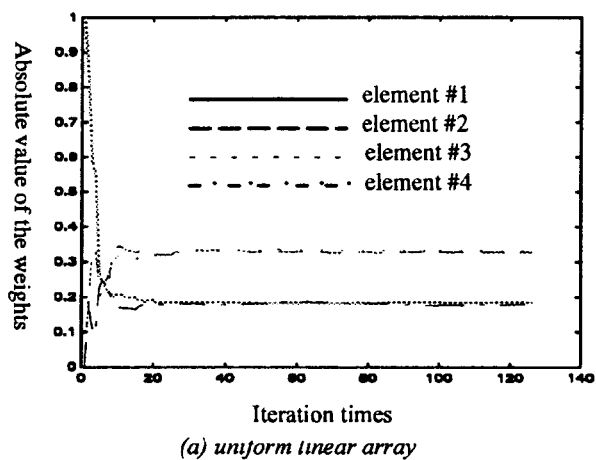


Fig. 1. The convergence of the RLS adaptive arrays.

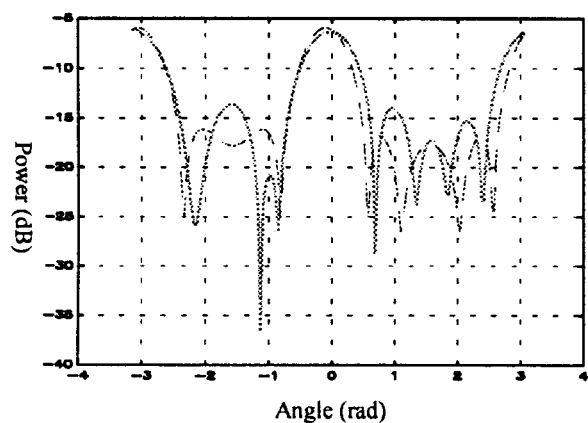


Fig. 2. Array pattern after RLS adaptation.
 — uniform circular array
 - - uniform linear array

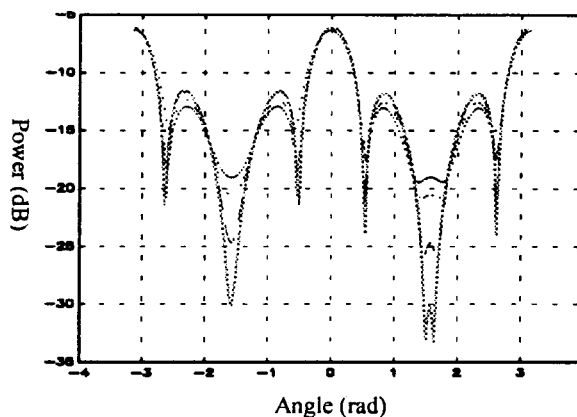


Fig. 3. Array pattern for ESPRIT array.

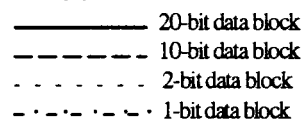


Fig. 4. Bit error rate performance.

